Title: Modelling *in vitro growth* of dense root networks

Running head: Modelling Growth of Hairy Roots

Corresponding author: M. Ptashnyk

Centre for Mathematical Biology

Mathematical Institute

24-29 St Giles'

Oxford OX1 3LB

UK

Tel.:+44 (0)1865 283891

Fax: +44 (0)1865 283882

e-mail: ptashnyk@maths.ox.ac.uk

Modelling *in vitro growth* of dense root networks

Peter Bastian[1], Andrés Chavarría-Krauser[23], Christian Engwer[1], Willi Jäger[2], Sven Marnach[1], Mariya Ptashnyk[24] *

[1] Institut für Parallele und Verteilte Systeme, Universität Stuttgart, Universitätsstraße 38, D-70569 Stuttgart, Germany

[2] Insitut für Angewandte Mathematik, Universität Heidelberg, INF 294, D-69120 Heidelberg, Germany

[3] Quantitative Analysis of Molecular and Cellular Biological Systems (BIOQUANT), Universität Heidelberg, INF 267, D-69120 Heidelberg, Germany

[4] Centre for Mathematical Biology, Mathematical Institute, University of Oxford, 24-29 St Giles', Oxford OX1 3LB, UK

*Corresponding author; e-mail: ptashnyk@maths.ox.ac.uk; Fax: +44 (0)1865 283882

Abstract

Hairy-roots are plants genetically transformed by *Agrobacterium rhizogenes*, which do not produce shoots and are composed manly by roots. Hairy-roots of *Ophiorrhiza mungos* Linn. are currently gaining interest of pharmacologists, since a secondary product of their metabolism, camptothecin, is used in chemotherapy. To optimize the production of valuable secondary metabolites it is necessary to understand the metabolism and growth of these roots systems. In this work, a mathematical model for description of apical growth of a dense root network (e.g. hairy-roots) is derived. A continuous approach is used to define densities of root tips and root volume. Equations are posed to describe the evolution of these and are coupled to the distribution of nutrient concentration in the medium and inside the network. Following the principles of irreversible thermodynamics, growth velocity is defined as the sum over three different driving forces: nutrient concentration gradients, space gradients and root tip diffusion. A finite volume scheme was used for the simulation and parameters were chosen to fit experimental data from *Ophiorrhiza mungos* Linn. hairy roots. Internal nutrient concentration determines short-term growth. Long-term behavior is limited by the total nutrient amount in the medium. Therefore mass yield could be increased by guaranteeing a constant supply of nutrients. Increasing the initial mass of inoculation did not result in higher mass yields, since nutrient consumption due to metabolism also rose. Four different growth strategies, are compared and their properties discussed.

This allowed to understand which strategy might be the best to increase mass production optimally. The model is able to describe very well the temporal evolution of mass increase and nutrient uptake. Our results provide further understanding of growth and density distribution of hairy root network and therefore it is a sound base for future applications to describe e.g. secondary metabolite production.

keywords: *growth model, nutrient uptake, hairy roots, transport equation, dense root network, continuous model*

1 Introduction

Plants remain a major source of pharmaceuticals and biochemicals. Many valuable phytochemicals, for example *camptothecin (Camptotheca acuminata)* used in chemotherapy, are secondary metabolites that are not essential to plant growth, they are produced in small amounts, and often accumulate in specialized tissues, e.g. trichome hairs (epidermal outgrowths). These compounds usually have very complicated structure and/or exhibit chirality. Consequently, in many cases organic synthesis is not cost effective, and extraction from field-grown plants is the major method used to produce these metabolites economically. Depending on the plant species, traditional agricultural methods often require months to years to be harvestable and levels of secondary metabolites can be affected by many factors, including pathogens and climate changes. Plant cell suspension cultures have therefore been considered as an alternative for producing valuable secondary metabolites (Kim *et al.* 2002; Kim *et al.* 2002).

Hairy root cultures, producing many of the same important secondary metabolites as the whole plant, are a potential means for producing valuable plant compounds, (Williams & Doran, 1999). Hairy roots are obtained through transformation by *Agrobacterium rhizogenes* and are special in the sense that these plants lack shoots and are composed mainly of a dense growing root system (Fig. 1). These roots can be cultivated under sterile conditions either in

a reactor or in shake flasks, (Singh & Curtis 1994; Tescione *et al.* 1997; Kim *et al.* 2003). The fast growing hairy roots are unique in their genetic and biosynthetic stability and are able to regenerate whole viable plants for further subculturing (Doran, 1997). Hairy roots thus provide also a good experimental system for studying root-specific pathways, (Flores *et al.*, 1999) and research on root metabolism, (Bais *et al.*, 2001), or rhizosphere (narrow zone surrounding the roots and being directly influenced by them), (Tepfer *et al.*, 1989).

Hairy roots of *Ophiorrhiza mungos* Linn., the Chinese camptotheca tree, are currently gaining the interest of pharmacologists, since a secondary metabolite, *camptothecin*, can be used to treat cancer diseases (Takimoto *et al.*, 1998). Campthothecin (CPT) is a modified monoterpene indole alkaloid produced by *Camptotheca acuminata*, *Nothapodytes foetida*, some species of the genus *Ophiorrhiza*, *Ervatamia heyneana*, and *Merrilliodendron megacarpum* (Sudo *et al.* 2002; Wink *et al.* 2005). In order to produce camptothecin efficiently, it is necessary to optimize the biological processes behind its biosynthesis (either in bioreactors or shaker cultures). However, to achieve this, it is essential to understand metabolism, growth and transport processes of and in root networks.

In the work presented here, a quantitative model of growth of these complicated root networks based on a continuous description using densities was derived by taking the main known biological properties of root growth into account. To show the capabilities of the model and to obtain estimates of the model parameters, simulations were compared to experimental data obtained from *O.*

mungos hairy roots grown as shaker cultures. Although the model was used to describe this special situation, it is general enough to describe other cultures and culture methods (such as bioreactors) with slight modification. In a long term it is desirable to understand growth and secondary metabolite production sufficiently well to optimize in vitro production of compounds such as CPT. As a first step towards this, we compare here four different growth strategies and discuss their properties. Depending on the chosen strategy, either wide spread or smaller packed root systems are predicted. Wide spread root tissues have the advantage of having better access to nutrients and oxygen and suffer thus less of nutrient depletion and anoxia, while densly packed root systems exploit space efficiently. It is a priori not clear which type of growth is optimal, as it depends on the type of growth system applied (bioreactor or shaker cultures) and has to be examined for each single case.

2 Derivation of model

Growth of single root tips is heterogeneously distributed along the organ axis (Erickson & Sax, 1956). These expand through cell elongation in the *elongation zone* and through cell division in the *meristem* (Beemster *et al.*, 2003). Several models describing the growth of a single root exist (see e.g. Silk *et al.* 1989; Morris & Silk 1992; Chavarría-Krauser & Schurr 2004; Chavarría-Krauser *et al.* 2005). Hairy roots, however, are composed of a dense

network of growing and branching root tips. On the one hand this fact makes it almost impossible to follow each tip. On the other hand, it allows to use a continuous description based on densities.

The elongation zone of root tips can be assumed to be small compared to the rest of the system. Therefore in the root system scale, growth of single roots can be assumed to be purely apical. This allows to use a similar approach as other authors have in the case of fungi mycelia and of blood vessels. In Edelstein & Segel 1983; Edelstein 1982; Edelstein-Keshet 1988 one dimensional models for fungi growth with constant growth velocity are presented. The equation for internal and external nutrient concentrations were coupled with growth equations via uptake, branching and metabolic degradation terms. The distinction between internal and external substrate allowed modelling of translocation inside the biomass network.

A more general growth model, which includes a mechanism that generates directed growth and allows description of mycelia growth in more than one spatial dimension, was proposed by Boswell *et al.* 2003. For detailed understanding of influence of heterogeneous environment on the development of each fungi hypha a discrete model was considered in Boswell *et al.* 2007. Growth of blood vessels, where the capillary sprout network is formed in response to external chemical stimuli, have also been described similarly (for both continuous and discrete models see e.g. Anderson & Chaplain 1998). All these approaches are similar and fit to some degree to the situation of root

networks. However, these need to be adapted and expanded to describe growing roots, which differ substantially from fungi hyphae and blood vessels. For example the model proposed by Boswell *et al.* 2003 focused on nutritional heterogeneity, which is probably the driving agent in mycelia expansion. For plant roots nutritional heterogeneity might be circumstantial, as other processes such as mechanical stresses, exudate production, or several tropisms such as hydrotropism, i.e. the tendency to follow gradients of water content, or gravitropism, i.e. growth towards direction of gravity, are also crucial. Therefore in the derivation of the hairy root growth model presented here, we use the known apical growth approach and take into account the biological properties of hairy roots by defining corresponding functions in the general framework.

2.1 Conservation of mass and root tips

Two densities suffice here to describe growth of hairy root networks. One is defined as the root volume per unit volume ($\rho = \rho(\vec{x}, t)$; given in $mm^3\, mm^{-3}$; $0 \leq \rho \leq 1$), while the other is defined as the cross section area of tips per unit volume ($n = n(\vec{x}, t) \geq 0$; given in $mm^2\, mm^{-3}$). For simplicity the root network is assumed to grow in a cuboid flask $\Omega \subset \mathbb{R}^3$, $\Omega = (0, l_w) \times (0, l_d) \times (0, l_h)$, where l_w, l_d and l_h are the length, depth and height of the cuboid, respectively. The total root volume contained in Ω will be denoted as $V_r(t) = \int_\Omega \rho(x, t)\, \mathrm{d}x$. The tip density n can also be given in number

of root tips per unit volume ($N = N(\vec{x}, t) \geq 0$; given in mm^{-3}).
Transformation is achieved through division of the areal density by the cross section area of one tip, $N = n/\pi r^2$, where r is the root radius assumed to be constant in the model. Growth can then be assumed to occur due to tip movement (elongation), tip formation (branching), and secondary growth, (Ninomiya *et al.* 2002; Kino-Oka *et al.* 1999). Growth rate depends on the nutrient concentration $c = c(t, \vec{x})$ (given in $mg\, mm^{-3}$) in the medium and on the internal nutrient concentration $\sigma = \sigma(t, \vec{x})$ (given in $mg\, mm^{-3}$), which is the amount of nutrient per unit root volume.

Tip movement and formation can be modeled as follows. The total tip cross section area contained in a *representative elementary volume* (REV; Bear 1972) $\omega \subset \Omega$ is given by $\int_\omega n \,\mathrm{d}x$. This total cross section area can only change by two ways, either the number of tips increases due to branching or tips move out of and/or into ω. Total branching can be modeled by $\int_\omega f \,\mathrm{d}x$, where f is a branching function which will be specified later in Eq. (3). Total flux is given by the integral of tip flux $n\vec{v}$ over the surface $\partial\omega$ of ω, i.e. $\int_{\partial\omega} n\, \vec{v} \cdot \vec{\nu} \,\mathrm{d}\varsigma$, where $\vec{\nu}$ is the outer normal vector of ω and $\vec{v}$ is the growth velocity of the tips. Therefore the change in time of the total tip cross section area in ω is given by

$$\frac{\mathrm{d}}{\mathrm{d}t} \int_\omega n \,\mathrm{d}x = -\int_{\partial\omega} n\, \vec{v} \cdot \vec{\nu} \,\mathrm{d}\varsigma + \int_\omega f \,\mathrm{d}x.$$

As ω does not change in time and using Gauss' integral formula the above expression becomes

$$\int_\omega \left(\partial_t n \,\mathrm{d}x + \nabla \cdot (n\, \vec{v}) - f\right) \mathrm{d}x = 0.$$

Since this expression holds for every volume ω, an equation describing the evolution and spatial distribution of n is obtained

$$\partial_t n + \nabla \cdot (n\,\vec{v}) = f \qquad \text{in } (0,T) \times \Omega \tag{1}$$

for some $0 < T < \infty$. Thus the change of n is defined by a transport equation with transport velocity $\vec{v}$ and a production term f. Eq. (1) needs suitable initial and boundary conditions to be solvable. The wall of the flask can be assumed to be impenetrable, which results in a *no-flux* condition $n\,\vec{v} \cdot \vec{\nu} = 0$ on the boundary $\partial\Omega$.

The change in volume density ρ is determined as follows. Assume again an REV $\omega \subset \Omega$. Per unit time a tip grows and displaces by the distance $\|\vec{v}\|$, so that per unit time a root volume of $\pi r^2 \|\vec{v}\|$ is produced, where πr^2 is its cross section area. Inside ω there is a cross section area per unit volume given by n, which corresponds to a certain amount of root tips per unit volume. Therefore root volume produced due to tips movement per unit time in ω is given by

$$\frac{\pi r^2}{\pi r^2} \int_\omega n \|\vec{v}\|\, dx = \int_\omega n \|\vec{v}\|\, dx \;,$$

where $\vec{v}$ is the average growth velocity in ω. This expression does not take processes into account, which do not depend directly on the average velocity $\vec{v}$. These processes are for example fluctuation of growth velocity within the population of root tips in ω and root thickening. We assume that these processes are described by a function q. Taking the above expression for the total volume production into account and that the total root volume in ω is given by

$V_r(\omega, t) = \int_\omega \rho \, \mathrm{d}x$, an equation for the change of root volume is obtained

$$\frac{\mathrm{d}V_r}{\mathrm{d}t}(\omega, t) = \frac{\mathrm{d}}{\mathrm{d}t} \int_\omega \rho \, \mathrm{d}x = \int_\omega n \, \|\vec{v}\| \, \mathrm{d}x + \int_\omega q \, \mathrm{d}x \, ,$$

Again ω was arbitrarily chosen and is independent of time. The above expression results thus in an equation describing the temporal evolution and spatial distribution of ρ

$$\partial_t \rho = n \, \|\vec{v}\| + q \qquad \text{in } (0, T) \times \Omega. \tag{2}$$

Similarly to Eq. (1), Eq. (2) needs a suitable initial condition to be solvable. Both initial conditions represent the act of inoculation into the medium. A small piece of hairy root material is needed to produce a new culture. This piece has a certain distribution of n and ρ, which correspond to the initial conditions. In contrast to Eq. (1), no boundary condition is needed here.

2.2 Growth functions

Eq. (1) and (2) contain the unknown functions f (branching function), $\vec{v}$ (growth velocity), and q (secondary growth). These functions depend on several variables and have to be postulated, as not much information is available about these dependencies.

Branching function

New root tips arise from root mass which is already present. Therefore f should depend on root density ρ. The nutrient concentration $c = c(t, \vec{x})$ (given in $mg\,mm^{-3}$) in the medium can be assumed to affect positively root branching (see e.g. Drew *et al.* 1973; Robinson 1994; Robinson 1996 for potassium, phosphate, nitrate, and ammonium). Moreover, branching costs energy and resources, which have to be provided by the root network. Therefore the function f is assumed to depend also on the internal nutrient concentration $\sigma = \sigma(t, \vec{x})$ (given in $mg\,mm^{-3}$; Kim *et al.* 2003; Schnapp *et al.* 1991). Since nutrient transport inside the root network is substantially faster in comparison to growth and branching, it is legitimate to assume that the model depends on the average internal nutrient concentration, $s(t) = V_r^{-1}(t) \int\limits_{\Omega} \sigma(t, \vec{x})\, \rho(t, \vec{x})\, \mathrm{d}x$ instead of the spatial heterogeneous σ. One possibility to define the translocation of nutrients inside the root network is to prescribe a diffusive and a chemotactic movement in the direction of the root tip, (see Boswell *et al.* 2003). In a tissue where density is maximal ($\rho = \rho_{max}$), branching is unlikely. Therefore f is assumed to be proportional to $\rho_{max} - \rho$. All three factors are assumed here to be limiting, so that the following branching function is proposed

$$f = \beta\, c\, s\, \rho\, (\rho_{max} - \rho)\ , \tag{3}$$

where β is a constant reflecting the sensibility of the branching rate to the internal and external nutrient concentrations.

Growth velocity and secondary thickening

Following the principles of irreversible thermodynamics average growth velocity $\vec{v}$ is proposed to be given by a weighted sum over general forces. In particular a hypothetical chemical potential μ is proposed to determine the average velocity

$$\vec{v} = R\, s\ (\rho_{max} - \rho)\ \nabla\mu\ ,$$

where R is a constant which reflects the sensitivity of growth towards the driving forces (will be denoted in the sequel as *growth rate coefficient*). The other factors are obtained similarly to the derivation of Eq. (1): growth is only possible when energy (internal substrate) is supplied to the tips (Kim *et al.* 2003; Schnapp *et al.* 1991); and $\vec{v}$ should be zero if a maximal root density is attained, i.e. when $\rho = \rho_{max}$.

As mentioned before, other processes which do not depend directly on $\vec{v}$ might be responsible for mass production and where taken into account by the function q [cmp. Eq. (2)]. This function is splitted into two parts, one represents the mass increase due to velocity fluctuation and the other by root thickening. The effect of velocity fluctuation can be assumed, similarly to $\vec{v}$, to be proportional to the internal nutrient concentration, to the space left for growing and to the density of root tips n, i.e. $n\, R\, s\ (\rho_{max} - \rho)\, \alpha_\tau$, where α_τ is a phenomenological constant characterizing the velocity fluctuation. Secondary thickening occurs to existing tissue and requires energy, therefore it is assumed to be proportional to

root density and internal nutrient concentration. We propose therefore

$$q = R\, s\, n\, (\rho_{max} - \rho)\, \alpha_\tau + \chi\, s\, \rho\, (\rho_{max} - \rho)\,, \tag{4}$$

where χ is a *secondary thickening rate*.

The idea behind the term describing the fluctuation of velocity is the following. It is possible that the root network grows and increases mass without a macroscopic gradient $\nabla\mu$ and without root thickening. Microscopically seen there exist always local gradients, which drive locally growth of the root tips (as long as there is space to grow). However, this property is lost during the transition from the microscale to the macroscale, because in this particular gedankenexperiment $\nabla\mu$ would be zero in first order. Therefore this local growth has to be included as an additional term.

Since hairy roots are agravitropic (Odegaard *et al.* 1997; Legue *et al.* 1996), μ can be assumed to be independent of gravity, so that the root tips are assumed to grow only along nutrient gradients and away from dense tissue. Under these circumstances, μ is proposed to be solely a function of c, ρ, and n, and its gradient be given by

$$\nabla\mu = \alpha_c\, \nabla c - \alpha_\rho\, \nabla\rho - \alpha_n\, \nabla n\,, \tag{5}$$

where α_c, α_ρ, α_n, are phenomenological constants, which are weights for each single growth strategy. The first term in (5) corresponds to the tendency of roots to grow towards higher nutrient concentrations. The second term reflects mechanical effects, i.e. growth towards free space, while the third term models

the tendency of tips to grow away from each other. The tendency of root tips to grow away from each other can be explained as follows. In the microscale root tips compete for nutrients and tend to grow away from each other, as nutrients are depleted locally by root tips. Moreover, root tips produce exudates which are believed to be involved in root-root signalling (Bais *et al.*, 2004). Local competition for nutrients and root-root communication cannot be described by the microscopic nutrient concentration. The simplest model to describe these processes is to assume a diffusion of tips. Altogether $\vec{v}$ is assumed to be given by

$$\vec{v} = R\, s\, (\rho_{max} - \rho)\, (\alpha_c \nabla c - \alpha_\rho \nabla \rho - \alpha_n \nabla n)\ . \tag{6}$$

2.3 Nutrient transport

Eqs. (3), (6), and (4) depend on medium and internal nutrients. The model describing the nutrient concentration in medium depends strongly on the experimental setup. This becomes clear by the number of models describing water and nutrient transport and uptake by single roots or plant root systems in unsaturated soil (Roose & Fowler 2004; Kim *et al.* 2004; Roose *et al.* 2001; Tinker & Nye 2000; Roose 2000; Barber 1995; Cushman 1984). The cultures modeled here were grown as shaker cultures. The flow produced by the shaking is complex, as it combines a free boundary and a porous medium (flow around the root network). Therefore the shaking is here accounted for by dispersion, which results in considerably larger diffusion/dispersion coefficients. The

volume occupied by the medium changes in time due to the increase in root volume. It is therefore not obvious how to pose the equation for conservation of nutrients.

External nutrients

Assume again a REV $\omega \subset \Omega$, which does not depend on time, but can be decomposed into two time dependent domains: $\omega = \omega_r(t) \cup \omega_m(t)$, where $\omega_r(t)$ and $\omega_m(t)$ are the volumes occupied by the roots and the medium, respectively. Instead of using the concentration c, which depends on $\omega_r(t)$, we choose the concentration $\mathcal{C} = (1-\rho)\, c$ which relates the nutrient content to the whole volume ω. Therefore the change in nutrient mass inside ω is given by

$$\frac{\mathrm{d}\mathcal{M}}{\mathrm{d}t} = \partial_t \int_\omega \mathcal{C}\, \mathrm{d}x = \int_\omega \partial_t \mathcal{C}\, \mathrm{d}x \; .$$

Remark here that it was essential that ω is time independent to apply the simple form of Leibniz's rule (therefore $\mathcal{C}$ was used instead of c). Else Reynold's transport theorem would have had to be applied, which would have resulted in an additional integral term over the boundary. Mass within ω can only change by means of a net flux through its boundary $\partial\omega$ and by uptake

$$\frac{\mathrm{d}\mathcal{M}}{\mathrm{d}t} = -\int_{\partial\omega} \vec{j} \cdot \vec{\nu}\, \mathrm{d}\varsigma - \int_\omega g\, \mathrm{d}x \; ,$$

where $g = g(c, n, \rho, s)$ is an *uptake function*. Using Gauss' theorem on the flux

term and equating the two expression for the mass change, we obtain

$$\int_\omega \left(\partial_t \mathcal{C} + \mathrm{div}\vec{j} + g\right)\, \mathrm{d}x = 0\,.$$

Here again ω was arbitrarily chosen, so that the expression inside the integral has to be zero. The flux density $\vec{j}$ has to be chosen phenomenologically. Molecular diffusion is driven by a gradient of chemical potential (Landau & Lifschitz 1991), which according to Fick's law is proportional to a gradient of concentration. The true local concentration, c, is relevant for the chemical potential and not $\mathcal{C}$. The area $\partial\omega$ is not completely permeable, as some of it, $\partial\omega_r(t)$, is occupied by roots. In the above derivation we included this fact into $\vec{j}$ and have to use therefore a dispersion coefficient dependent on ρ. Altogether we choose $\vec{j} = -\mathcal{D}_c(\rho)\nabla c$, where $\mathcal{D}_c = \mathcal{D}_c(\rho)$ is a non constant dispersion coefficient. Using the definition of $\mathcal{C}$, we find finally

$$\partial_t((1-\rho)c) - \nabla\cdot(\mathcal{D}_c(\rho)\nabla c) \;=\; -g \qquad \text{in} \quad (0,T)\times\Omega\,, \tag{7}$$

$\mathcal{D}_c$ depends on the root density ρ and should be zero when $\rho = 1$ (no space for dispersion to take place). Therefore $\mathcal{D}_c$ is proposed to be $\mathcal{D}_c(\rho) = D_c\ (1-\rho)$, where D_c is a constant. Nutrient uptake occurs on the root surface near the tips. Thus the uptake function g is assumed to be proportional to root volume density and root tip density. Two sorts of nutrient transport are feasible on the root surface, active and passive transport. Active transport is assumed to be unidirectional (into the root network) and dependent only on the local medium nutrient concentration c. Passive transport depends on the nutrient gradient

between medium and roots, on the difference $c - s$. Thus, the nutrient uptake function g is proposed to have the form

$$g(c, n, \rho, s) \;=\; \frac{2\lambda\, n}{r}\, \rho\, \left(K_m(s)\, c + P\, (c - s) \right) \,, \tag{8}$$

where λ is the characteristic length of the uptake-active tissue around a tip ($\frac{2\lambda\, n}{r}$ is the uptake surface density), $K_m(s)$ is a uptake rate, and P is a permeability. Eq. (7) needs also suitable initial and boundary conditions. At the beginning of an experiment the medium is well stirred and a constant homogeneous distribution of nutrients can be assumed to exists. The walls of the flask are assumed to be impermeable to the medium, therefore no-flux conditions are considered $\nabla c \cdot \vec{\nu} = 0$ on $\partial\Omega$.

Internal nutrients

In contrast to the medium nutrient concentration, a spatial average is used for the internal nutrient concentration s (spatial distribution of the nutrient inside the network is neglected). Four processes which change the internal concentration are considered here: uptake, growth, branching and metabolism. For the total internal concentration $S = s\, V_r = \int\limits_{\Omega} \sigma(t, \vec{x}) \rho(t, \vec{x})\, \mathrm{d}x$, the following equation is proposed

$$\frac{\mathrm{d}}{\mathrm{d}t} S \;=\; \int\limits_{\Omega} g\, \mathrm{d}x - \gamma_g \int\limits_{\Omega} \left(n\, \|\vec{v}\| + q \right)\, \mathrm{d}x - \gamma_r \int\limits_{\Omega} f\, \mathrm{d}x - \gamma_m\, S \,, \tag{9}$$

where γ_g, γ_r and γ_m are constants describing the proportion of metabolites used for growth, branching and metabolism, respectively. To solve Eq. (9), an initial

condition $S = S_0$ is needed. This condition describes the initial total amount of nutrients in the inoculum.

2.4 Complete model

Altogether the complete model of hairy root growth reads

$$
\begin{aligned}
&\partial_t n + \nabla \cdot (n\,\vec{v}) = f && \text{in } (0,T)\times\Omega,\\
&\partial_t \rho = n\,\|\vec{v}\| + q && \text{in } (0,T)\times\Omega,\\
&\partial_t\left((1-\rho)c\right) - \nabla\cdot(D_c(1-\rho)\nabla c) = -g && \text{in } (0,T)\times\Omega,\\
&\tfrac{\mathrm{d}}{\mathrm{d}t}S = \int\limits_\Omega g\,\mathrm{d}x - \gamma_g \int\limits_\Omega (n\,\|\vec{v}\| + q)\;\mathrm{d}x - \gamma_r \int\limits_\Omega f\,\mathrm{d}x - \gamma_m\,S && \text{in } (0,T),
\end{aligned}
\tag{10}
$$

with

$$
\begin{aligned}
\vec{v} &= \frac{R\,S}{V_r}\,(\rho_{max}-\rho)(\alpha_c\nabla c - \alpha_\rho\nabla\rho - \alpha_n\nabla n)\;,\\
f &= \frac{\beta\,c\,S\,\rho}{V_r}\,(\rho_{max}-\rho)\;,\\
q &= \frac{R\,S\,n}{V_r}\;(\rho_{max}-\rho)\,\alpha_\tau + \frac{\chi\,S\,\rho}{V_r}\,(\rho_{max}-\rho)\;,\\
g &= \frac{2\lambda\,n}{r}\,\rho\,(\,K_m(\frac{S}{V_r})\,c + P\,(c - \frac{S}{V_r}))\;,\\
V_r &= \int_\Omega \rho\,\mathrm{d}x\;.
\end{aligned}
$$

The initial and boundary conditions are

$$
\begin{aligned}
\rho(0,\vec{x}) &= \rho_0\,\phi(\vec{x}) && \text{in} \quad \Omega,\\
n(0,\vec{x}) &= n_0\,\phi(\vec{x}) && \text{in} \quad \Omega,\\
c(0,\vec{x}) &= c_0 && \text{in} \quad \Omega,\\
S(0) &= S_0,\\
n\,\vec{v}\cdot\vec{\nu} &= 0 && \text{on} \quad \partial\Omega\times(0,T),\\
\nabla c\cdot\vec{\nu} &= 0 && \text{on} \quad \partial\Omega\times(0,T)\ ,
\end{aligned}
$$

where ϕ is an initial spatial distribution. If in growth velocity $\vec{v}$ the constant α_ρ or α_n is non-zero we obtain a diffusive term in the equation for n and the boundary condition $n\,\vec{v}\cdot\vec{\nu}=0$ is well-posed. In another case the zero-flux boundary condition for c will imply the well-posedness of the boundary condition for n.

3 Materials and Methods

The numerical solution of the model will be compared with the experimental data obtained from *O. mungos* (B. Wetterauer and M. Wink, IPMB, Universität Heidelberg, unpublished). The hairy root cultures were cut to have an initial weight of approximately 1.78 ± 0.1 g (25 values) and were grown in a shaker flask in the dark for 4 weeks (ca. 672 hours). The initial concentration of

sucrose in the medium was set to $c_0 = 11.46\ g\,l^{-1}$. The main purpose of the shaking of the cultures is to ensure distribution of nutrients and oxygen, this means that transport of sucrose in the medium is non-limiting to uptake and hence to growth. After 2 weeks (ca. 336 hours) the cultures were transferred into fresh medium (again of concentration $11.46\ g\,l^{-1}$) and cultured in the same conditions for the following 2 weeks. Roots were harvested every one, two or four days, at 25, 50.5, 96, 144, 240.5, 336, 360, 384.5, 432, 480.5, 581.5, 671.75 hours (two cultures per harvest). Fresh weight, dry weight, and nutrient concentration were measured. Due to the lack of shoots and the absence of photosynthesis in hairy roots, the medium for cultivation has to contain sucrose as the main nutrient for growth, (Kim *et al.* 2003; Kim *et al.* 2002).

4 Simplifications, parameters and initial conditions

For numerical simulation and model calibration Eq. (10) was simplified to reduce the number of free parameters. Uptake of nutrients was considered to be purely of active nature, neglecting the passive transport ($P = 0$). The uptake rate K_m was assumed to be constant and independent of s. Moreover, the energy cost for branching of new tips was neglected ($\gamma_r = 0$). Since the root branches are very thin ($133 \pm 7\ \mu m$, 12 roots) and the variations of radius r are small, root thickening (secondary growth) can be neglected ($\chi = 0$) as well.

Experiments conducted on *O. mungos* showed that vertical growth is very small, i.e. growth occurs almost radially. This is a consequence of the experimental setup. The height of the medium is kept small to avoid anoxia and the roots do not grow beyond the boundary of the medium. Therefore the solution of the model can be assumed to be constant in vertical direction and the third dimension can be neglected in Eq. (10).

Sucrose was selected here as the growth limiting nutrient in the model. A homogeneously distributed initial concentration c_0 was considered for simulation. As already mentioned, in the experiments cultures were transferred into fresh medium after ca. $336\ h$, to guarantee viable growth of the cultures for 4 weeks. The dimensions of the flask ($l_w = 70$ mm, $l_d = 70$ mm and $l_h = 10$ mm) were chosen to have the same medium volume used in the experiments (ca. 49 ml), resulting in the same total amount of sucrose. For simplicity, the tissue was assumed to have an initial internal nutrient concentration $S_0 = 0$. The diffusion coefficient of sucrose in water at a temperature of 25° C is $1.88\,\text{mm}^2\text{h}^{-1}$ (Nobel, 1999). However, the shaking of the cultures produces a substantially higher dispersion coefficient. D_c was varied until it became non-limiting to growth ($D_c = 35$ mm^{2}h^{-1}).

The initial root volume and tip density distributions ($\rho(0, \vec{x})$ and $n(0, \vec{x})$, respectively), were chosen to be radially symmetric and given by a smooth

function $\phi(\vec{x}) = (1 - \tanh(\|\vec{x} - \vec{x_0}\| - r_{max})/2)/2$, where $\vec{x_0}$ is the center of the flask. Radius r_{max} was determined according to the experimentally determined initial root density $\rho_0 = 0.5\,\text{mm}^3\text{mm}^{-3}$ and root weight $M_0 = 1.78$ g through the equation $r_{max} = \sqrt{10^3\, M_0/(\pi l_h \rho_0)}$, $[r_{max}] =$ mm, where $[\cdot]$ denote the units of the variable.

Although here radially symmetric initial conditions were chosen and in principle the equations become 1D. In this particular case it is possible to simplify Eqs. (10), which contain then only partial derivatives in time and in radial direction, these stay however non-linear. The true improvement behind these simplification, would be the possibility to use numerical schemes, that are simpler to implement. This, of course, at the expense of not being able to simulate more complex situations, which might be necessary for example in bioreactor applications. The here presented model and algorithms are general enough to describe such applications.

The root tissues were observed not to be more dense than 0.7 mm^{3}mm^{-3}, therefore a maximal root density $\rho_{max} = 0.7\,\text{mm}^3\text{mm}^{-3}$ was chosen here. For the sake of simplicity instead of prescribing n_0 directly, it is easier to prescribe the initial number of tips per unit volume N_0 ($n_0 = N_0\,\pi r^2$, $[N_0] = \text{mm}^{-3}$). N_0 was not available experimentally, thus N_0 had to be estimated from the data by fitting of the mass change and nutrient uptake kinetics. For simplicity, the root radius was set to be $r = 0.1$ mm and the uptake-active zone behind the root tips was chosen to be $\lambda = 1$ mm long. The remaining parameters were selected

manually such that the numerical results fit the experimental data obtained from *O. mungos* (cmp. Table I). Rough estimates of the parameters were initially selected and used to simulate the model. Using this solution, the coefficient of determination, R^2, was calculated by comparison with measurements of both total nutrient concentration and biomass (cmp. Figs 2 a,b). The parameters were adapted and the process was iteratively continued until the R^2 values were maximized.

5 Numerical methods

The model (10) was simulated using a personal computer. The implementation is based on the DUNE framework (Bastian *et al.* (2004), http://www.dune-project.org/). For spatial discretization of the first and third equation in (10) a cell centered finite volume scheme on a structured grid was used, as described in LeVeque (2002). Finite volume schemes feature local mass conservation, which is essential for the comparison with experimental data. For the time discretization the diffusive part and the convective/reactive part of the equation were decoupled, using second order operator splitting introduced by Strang 1968. To prevent both instabilities in the transport term and effects from strong numerical diffusion, the convection equation was solved using an explicit second order Godunov upwind scheme with a minmod slope limiter (Sweby, 1984; LeVeque, 2002). To obtain a stable solution,

discretization in time was chosen to fulfill the Courant-Friedrichs-Lewy condition (Courant *et al.*, 1928). The diffusive part of the equation was solved using the implicit Euler method. The equations for the root density and the inner nutrient concentration S [second and forth equation in (10)] were solved with an explicitly Euler scheme (Stoer & Burlisch, 2000). Similar to the determination of total mass increase and nutrient concentrations (inner and medium), coupling between the spatial distributions [i.e. $\rho(t, \vec{x})$, $n(t, \vec{x})$ and $c(t, \vec{x})$] and the inner nutrient concentration S was achieved using numerical integration.

6 Results and Discussion

The capabilities of the model are demonstrated here by comparison to experimental data obtained from *O. mungos* hairy roots grown as shaker cultures. The kinetics of growth and medium nutrient (sucrose) concentration obtained in the experiments are compared to the simulation results in Figs. 2 a,b. Very good agreement between the experimental data and numerical solution was found. This is reflected in the corresponding R^2 values (root mass: $R^2 = 0.85$; nutrient concentration in medium: $R^2 = 0.93$). The numerical solution for the root tip density and concentration of nutrients inside the roots is illustrated in Fig. 2 c.

The inner nutrient concentration (Fig. 2 c) and the mass kinetics (Fig. 2 a) show that mass increase was limited directly by nutrient availability inside the

network. However, the medium concentration (Fig. 2 b) determined overall long-term growth. Variations of medium concentration were buffered by the possibility of the root network to accumulate nutrients. This is reflected by a high internal nutrient concentration in comparison to the external concentration (Fig. 2 c). Within the first $150\ h$ the network had to build a reservoir of inner nutrients. This could occur only if sufficient root tips existed to acquire the nutrients. This resulted therefore in a higher branching rate (Fig. 2 c) and a moderate mass increase (Fig. 2 a). After an initial production of root tips, internal nutrients reached a maximum concentration (at ca. $120\ h$). These nutrients were used to increase mass, which explains why growth per unit time was at that moment very high (Fig. 2 a). After $120\ h$ metabolism started to dominate, which is reflected in a reduction of both internal concentration and mass increase, although the medium still had enough nutrients (Fig. 2 b). The medium nutrient concentration fell continuously and became limiting to mass increase and branching rate (Figs. 2 a-c). Growth ceased until new medium was supplied at $336\ h$. The culture then grew again until the new nutrients were consumed.

Fig. 3 shows the spatial distribution of volume density (a), root tip density (b), nutrient concentration in medium (c) and local mass increase (d) after $380\ h$ of growth. Gradients of nutrients and tip density were chosen here as the driving force of growth (Table I). Density ρ increased from an initial value of $0.5\ mm^3mm^{-3}$ to almost $\rho_{max} = 0.7\ mm^3mm^{-3}$ and showed a distribution

with compact tissue in the center and less compact tissue towards the edge (Fig. 3 a). Mass increase was therefore due to both increase in tissue density and tissue expansion. Growth around the center originated from increase in tissue density due to velocity fluctuations [cmp. Eqs. (2) and (4)], while expansion around the edge occurred due to gradient growth [cmp. Eq. (6)]. The root tip density showed a distribution with a flat maximum and fell in waves with increasing distance from the center (Fig. 3 b). The existence of a maximum root tip density in the center is a consequence of the first $150\ h$ of growth, in which root tips had to be produced to increase nutrient uptake. This tips could not grow away from the center because $\nabla\mu \approx 0$ there. The waves were a consequence of the nutrient concentration changing in time. Nutrient concentration showed, as expected, small spatial variation outside the tissue (Fig. 3 c). Transport and uptake depend on the root density [$\mathcal{D}_c \propto (1-\rho)$; $g \propto \rho$; compare Eq. (7)], which is spatially inhomogeneous, thus a non-constant reduction of concentration was found where $\rho \neq 0$. Mass increase was as expected radially symmetric and occurred in a more or less *shock*-like manner (Fig. 3 d). A front of growth moved away from the tissue's center. It is also very clear that in the center of the tissue mass increase was at this moment almost zero, because the volume density was already close to ρ_{max}.

Using numerical simulations the influence of parameters on the solution of the model can be examined. In Figs. 4 a-d the solutions for different values of the most important parameters, namely branching rate and growth rate coefficient,

are presented. From all parameters, only one was varied and the other were kept constant (values listed in Table I). The branching rate β was varied from 25 to 65 mm^{-1} h $^{-1}$ mm^{6} mg^{-2}, while the growth rate coefficient R was varied from 6 to 14 mm h^{-1} mm^{3} mg^{-1}. Mass increase is influenced positively by β mostly due to the higher amount of root tips which ensure a faster assimilation of nutrients (Fig. 4 a,b). As expected, an increase in R increments also mass production (Fig. 4 c). However, nutrient uptake is almost not influenced by R (Fig. 4 d).

Cutting a root tissue to obtain an exact initial mass in an experiment is almost impossible. The dependency of the model on a varying initial root mass is thus also of interest (Figs. 5 a,b). Moreover, the initial tip density was not determined experimentally and was empirically determined in the model. It was thus important to understand the influence of this parameter on the simulation results (Fig. 5 c,d). The initial mass M_0 was varied from 0.5 to 2.9 g, while values from 0.5 to 6.0 mm^{-3} were used for the initial tip density N_0. The initial differences in M_0 become smaller due to the higher metabolism of the heavier cultures (Fig. 5 a). It is interesting that nutrient uptake depends on M_0 almost only in the first $336\ h$ (Fig. 5 b). After supplementation of fresh nutrients, almost no difference is found in the uptake rate. This can be explained by a small effect of initial mass on the root tip density, which is crucial for uptake (compare Fig. 4 b). Variation of N_0 affected the time needed by the tissue to acquire enough nutrients for growth (Fig. 5 c). Growth starts sooner when N_0 is

larger. However, no large impact on final mass is found. Similar to the case of M_0, not much influence on nutrient uptake is found after supplementation of fresh medium (Fig. 5 d). Both variations of M_0 and N_0 show that the model is self-regulating. Although growth and uptake kinetics depend on these initial values, similar final masses are obtained. Therefore neither the initial mass nor the root tip density can be used to increase yield substantially.

Although a simple method exists to estimate roughly the spatial distribution of mass by taping the roots on paper and cutting and weighting the paper, it is not clear if this would be exact enough to differ between different growth strategies. Moreover, these differ also in the distribution of root tip density, which could only be determined cumbersomely by manual counting of tips using a microscope. Therefore no experimental data which gives information on the spatial distributions is available to the authors. It is not clear which growth process dominates. Do hairy roots follow rather nutrient gradients than space gradients, or is the diffusion of root tips more important? Or is mass increase a consequence of increase in tissue density? It will probably be a mixture of all and other processes not accounted for. For the above simulations and fitting of the model, a mixture between nutrient and root tip density gradients was chosen. However, it is for further research interesting to understand the differences between possible combinations.

Figs. 6 a,b shows the distributions ρ and n when growth was driven solely by gradients of tip density ($\alpha_n = 1$, $\alpha_\rho = \alpha_c = \alpha_\tau = 0$). The center of the tissue is

less compact, while around the center a ring with $\rho \approx \rho_{max}$ is present. Towards the edge of the tissue, ρ falls smoothly (Fig. 6 a). Root tip density N has a distinct maximum and falls smoothly towards the edge (Fig. 6 b), in contrast to the flat maximum and wave-like structure found in the standard case (Fig. 3 b). A completely different type of growth was found when mechanical effects were chosen to be dominant ($\alpha_\rho = 1$, $\alpha_n = \alpha_c = \alpha_\tau = 0$; Figs. 6 c,d). Again as in the standard case a smooth ρ distribution is found (Fig. 6 c). However maximal density ρ_{max} is not reached and mass increase occurred mostly due to tissue expansion. The root tip density shows a flat maximum, falls however steeply and has a corona (Fig. 6 d). In the center many root tips were "trapped" by the low driving gradient $\nabla\rho \approx 0$. However, a shock-like wave of root tips grew away from the center building the corona around the maximum (Fig. 6 d). Figs. 6 e,f present the distributions for the case where growth is given only by fluctuations of growth velocity (pure increase in density of tissue; $\alpha_\tau = 1/9$, $\alpha_\rho = \alpha_c = \alpha_n = 0$). In contrast to the other cases, mass increase is determined completely by increase of tissue density (6 e). Therefore mass increase is limited by maximal possible volume density ρ_{max} and by the initial size of the tissue. The density of root tips N has a local minimum in the center of the tissue, which arises from the factor ($\rho_{max} - \rho$) in the branching function f.

From these three cases, the cases where root tip diffusion ($\alpha_n = 1\ mm^2$) and space gradients ($\alpha_\rho = 1\ mm$) drive growth are optimal to obtain nutrients. Through increase of perimeter of the tissue, a large surface with access to fresh

nutrients is achieved. When space gradients drive growth, the tissue is less compact than in the other cases. This allows a better distribution of nutrients between the roots, enhancing uptake. However, many root tips are “trapped” in the center of the tissue, where less nutrients are available and lose their uptake function almost completely. This situation is less pronounced but still present when tip diffusion drives growth. Although the contact surface between fresh nutrients and tissue is large in these cases, the ratio between perimeter and volume becomes smaller for increasing radius. On the one hand, this ratio is optimal when tissue density increase ($\alpha_\tau = 1/9$) is responsible for mass increase. But on the other hand, the tissue cannot exploit this advantage, as possible mass increase is bounded from the beginning. Pure increase in tissue density is optimal in exploiting mass production per unit volume of tissue. Root with $\alpha_c = 0$ would not be able to follow nutrient gradients, which would be an enormous disadvantage in heterogeneous environments. The standard case ($\alpha_c = 500\ mm^4 mg^{-1}$, $\alpha_n = 0.5\ mm^2$ and $\alpha_\tau = 1/9$), i.e. growth driven by concentration gradients and root tip diffusion with moderate increase in tissue density, seems to be optimal in combining all good properties mentioned above.

The model is able to describe very well the mass increase and uptake kinetics (Figs. 2 a,b). To understand which type of growth dominates in hairy roots, further experiments investigating this issue are required. Figs. 3 and 6 are a good reference to achieve this. The model is a good starting point to model metabolite production, e.g. of camptothecin. It opens also the possibility to test

several hypothesis within a short time and to determine where the processes could be optimized. This would require substantially more time if a pure experimental approach would be used.

Acknowledgments

The authors wish to thank Bernhard Wetterauer, Jenny Bauer, Michael Wink, and Tiina Roose. This work was supported by the BMBF-project “Modellierung, Simulation und Optimierung von Hairy-Root-Reaktoren” (03BANCHD) and by the “Center for Modelling and Simulation in the Biosciences“ (BIOMS) PostDoc program.

References

Anderson, A. R. A. & Chaplain, M. A. J. ,1998. Continuous and discrete mathematical models of tumor-induced angiogenesis. Bulletin of Mathematical Biology, 60, 857–900.

Bais, H. R., Loyola-Vargas, V. M., Flores, H. E. & Vivanco, J. M. ,2001. Root specific metabolism: the biology and biochemistry of underground organs. In Vitro Cell Dev. Biol..–Plant, 37, 730–741.

Bais, H. R., Park, S. W., Weir, T. L., Callaway, R. M. & Vivanco, J. M. ,2004.

How plants communicate using the underground information superhighway. Trends in PLant Science, 9, 26–32.

Barber, S. A. ,1995. Soil nutrient bioavailability: a mechanical approach. Wiley-Sons, Inc., New York.

Bastian, P., Droske, M., Engwer, C., Klöfkorn, R., Neubauer, T., Ohlberger, M. & Rumpf, M. ,2004. Towards a unified framework for scientific computing. In *Domain Decomposition Methods in Science and Engineering*, (Kornhuber, R., Hoppe, R., Keyes, D., Périaux, J., Pironneau, O. & Xu, J., eds), number 40 in Lecture Notes in Computational Science and Engineering pp. 167–174, Springer-Verlag.

Bear, J. ,1972. Dynamics of Fluids in Porous Media. Elsevier, New York.

Beemster, G. T. S., Fiorani, F. & Inzé, D. ,2003. Cell cycle: the key to plant growth control? TRENDS in Plant Science, 8 (4), 154–158.

Boswell, G. P., Jacobs, H., Davidson, F. A., Gadd, G. M. & Ritz, K. ,2003. Growth and function of fungal mycelia in heterogeneous environments. Bulletin of Mathematical Biology, 65, 447–477.

Boswell, G. P., Jacobs, H., Ritz, K., Gadd, G. M. & Davidson, F. A. ,2007. The development of fungal networks in complex environments. Bulletin of Mathematical Biology, 69, 605–634.

Chavarría-Krauser, A., Jäger, W. & Schurr, U. ,2005. Primary root growth: a

biophysical model of auxin-related control. Functional Plant Biology, 32 (9), 849–862.

Chavarría-Krauser, A. & Schurr, U. ,2004. A cellular growth model for root tips. Journal of Theoretical Biology, 230 (1), 21–32.

Courant, R., Friedrichs, K. & Lewy, H. ,1928. Über die partiellen Differenzengleichungen der mathematischen Physik. Mathematische Annalen, 100, 32–74.

Cushman, J. H. ,1984. Nutrient transport inside and outside the root rhizosphere; generalized model. Soil Science, 138 (2), 164–171.

Doran, P. M. ,1997. Hairy Roots: Culture and Applications. Harwood Academic Publishers, Amsterdam.

Drew, M. C., Saker, L. R. & Ashley, T. W. ,1973. Nutrient supply and the growth of the seminal root system in barley. Journal of Experimental Botany, 24, 1189–1202.

Edelstein, L. ,1982. The propagation of fungal colonies: a model for tissue growth. Journal of Theoretical Biology, 98, 679–701.

Edelstein, L. & Segel, L. A. ,1983. Growth and metabolism in mycelial fungi. Journal of Theoretical Biology, 104, 187–210.

Edelstein-Keshet, L. ,1988. Mathematical models in biology. The Random House/ Birkhäuser Mathematics Series, New York,.

Erickson, R. O. & Sax, K. W. ,1956. Experimental growth rate of primary root of *Zea mays*. Proceedings of the American Philosophical Society, 100, 487–498.

Flores, H. E., Vivanco, J. M. & Loyola-Vargas, V. M. ,1999. Radicle biochemistry: the biology of root-specific metabolism. Trends Plant Sci. 4, 220–226.

Kim, J., Sung, K., Corapcioglu, M. Y. & Drew, M. C. ,2004. Solute transport and extraction by a single root in unsaturated soils: model development and experiment. Environmental Pollution, 131, 64–70.

Kim, Y. J., Weathers, P. J. & Wyslouzil, B. E. ,2002. Growth of *Artemisia annua* hairy roots in liquid and gas-phase reactors. Biotechnology and Bioengineering, 80, 454–464.

Kim, Y. J., Weathers, P. J. & Wyslouzil, B. E. ,2003. Growth dynamics of *Artemisia annua* hairy roots in three culture systems. Journal of Theoretical Biology, 83, 428–443.

Kim, Y. J., Wyslouzil, B. E. & Weathers, P. J. ,2002. Invited review: secondary metabolism of hairy root cultures in bioreactors. In Vitro Cell. Dev. Biol. Plant, 38, 1–10.

Kino-Oka, M., Hitaka, Y., Taya, M. & Tone, S. ,1999. High-density culture of red beet hairy roots by considering medium flow condition in a bioreactor. Chemical Engineering Science, 54, 3179–3186.

Landau, L. D. & Lifschitz, E. M. ,1991. Hydrodynamik. 5. edition, Akademie Verlag, Berlin.

Legue, V., Driss-Ecole, D., Maldiney, R., Tepfer, M. & Perbal, G. ,1996. The response to auxin of rapeseed (*Brassica napus* L.) roots displaying reduced gravitropism due to transformation by *Agrobacterium rhizogenes*. Planta, 200, 119–124.

LeVeque, R. J. ,2002. Finite Volume Methods for Hyperbolic Problems. Cambridge University Press.

Morris, A. K. & Silk, W. K. ,1992. Use of a flexible logistic function to describe axial growth of plants. Bulletin of Mathematical Biology, 54, 1069–1081.

Ninomiya, K., Kino-Oka, M., Taya, M. & Tone, S. ,2002. Segmental distribution in potentials of lateral root budding and oxygen uptake of plant hairy roots. Biochemical Engineering Journal, 10, 73–76.

Nobel, P. S. ,1999. Physicochemical & Environmental Plant Physiology. Academic Press, San Diego.

Odegaard, E., Nielsen, K. M., Beisvag, T., Evjen, K., Johnsson, A., Rasmussen, O. & Iversen, T. H. ,1997. Agravitropic behaviour of roots of rapeseed (*Brassica napus* L.) transformed by *Agrobacterium rhizogenes*. J Gravit Physiol. 4 (3), 5–14.

Robinson, D. ,1994. Tansley review no. 73. The responses of plants to non-uniform supplies of nutrients. The New Phytologist, 127, 635–674.

Robinson, D. ,1996. Resource capture by localized root proliferation : Why do plants bother? Annals of Botany, 77, 179–185.

Roose, T. ,2000. Mathematical model of plant nutrient uptake. PhD Thesis, Oxford.

Roose, T. & Fowler, A. C. ,2004. A mathematical model for water and nutrient uptake by plant root systems. Journal of Theoretical Biology, 228, 173–184.

Roose, T., Fowler, A. C. & Darrah, P. R. ,2001. A mathematical model of plant nutrient uptake. Journal Math. Biology, 42, 347–360.

Schnapp, S. R., Curtis, W. R., Bressan, R. A. & Hasegawa, P. M. ,1991. Growth yields and maintenance coefficients of unadapted and NaCI-adapted tobacco cells grown in semicontinuous culture. Plant Physiol, 96, 1289–1293.

Silk, W. K., Lord, E. M. & Eckard, K. J. ,1989. Growth pattern inferred from anatomical records. Plant Physiology, 90, 708–713.

Singh, G. & Curtis, W. R. ,1994. Reactor design for plant root culture. Boca Raton, FL, pp. 185–206.

Stoer, J. & Burlisch, R. ,2000. Numerische Mathematik 2. 4 edition, Springer.

Strang, G. ,1968. On the construction and comparison of difference schemes. SIAM J. Numer. Anal. 5, 506–517.

Sudo, H., Yamakawa, T., Yamazaki, M., Aimi, N. & Saito, K. ,2002. Bioreactor production of camptothecin by hairy root cultures of *Ophiorrhiza pumila*. Biotechnology Letters, 24, 359–363.

Sweby, P. K. ,1984. High resolution schemes using flux-limiters for hyperbolic conservation laws. SIAM J. Num. Anal. 21, 995–1011.

Takimoto, C. H., Wright, J. & Arbuck, S. G. ,1998. Clinical applications of the camptothecins. Biochim Biophys Acta, 1400, 107–119.

Tepfer, D., Metzger, L. & Prost, R. ,1989. Use of roots transformed by *Agrobacterium rhizogenes* in rhizosphere research: applications in studies of cadmium assimilation from sewage sludges. Plant Molecular Biology, 13, 295–302.

Tescione, L. D., Ramakrishnan, D. & Curtis, W. R. ,1997. The role of liquid mixing and gas-phase dispersion in a submerged, sparged root reactor. Enzyme Microb. Technol. 20, 207–213.

Tinker, P. B. & Nye, P. H. ,2000. Solute movement in the rhizosphere. Oxford University Press, New York, Oxford.

Williams, G. R. C. & Doran, P. M. ,1999. Investigarion of liquid-solid hydrodynamic boundary layers and oxygen requirements in hairy root cultures. Biotechnology and Bioengineering, 64 (6), 729–740.

Wink, M., Alfermann, A. W., Franke, R., Wetterauer, B., Distl, M., Windhövel, J., Krohn, O., Fuss, E., Garden, H., Mohagheghzadeh, A., Wildi, E. & Ripplinger, P. ,2005. Sustainable bioproduction of phytochemicals by plant in vitro cultures: anticancer agents. Plant Genetic Resources. NIAB. 3(2), 90–100.

Table I. Model parameters used for simulation.

Prescribed parameters		Fitted parameters	
$\lambda\ (mm)$	1	$R\ (mm\,h^{-1}\,mm^3\,mg^{-1})$	10
$r\ (mm)$	0.1	$\beta\ (h^{-1}\,mm^{-1}\,mm^6\,mg^{-2})$	45
$D_c\ (mm^2\,h^{-1})$	35	$K_m\ (mm\,h^{-1})$	0.08
$\alpha_c\ (mm^4\,mg^{-1})$	500	$\gamma_g\ (mg\,mm^{-3})$	0.005
$\alpha_\rho\ (mm)$	0	$\gamma_m\ (h^{-1})$	0.02
$\alpha_n\ (mm^2)$	0.5		
α_τ	$\frac{1}{9}$		
$P(mm\,h^{-1})$	0		
$\gamma_r(mg\,mm^{-2})$	0		
$\chi(mm^3\,mg^{-1}\,h^{-1})$	0		

List of Figures

(c,d). The other parameters were kept constant. Increase of R or β result in similar increase of root mass. Increase of R has however almost no effect on the kinetics of nutrient uptake, in contrast to β.

5 Simulation of mass increase and medium nutrient concentration for variable initial root mass M_0 (a,b) and variable initial tip density N_0 (c,d). The other parameters were kept constant. N_0 is given in number of tips per unit volume. The advantage of higher initial root mass and root tips density was temporary and decreased in time.

6 Simulated spatial distribution of root volume and root tip densities after $380\ h$ of growth for different growth strategies. (a) and (b) ρ and N for root tip density gradient driven growth ($\alpha_n = 1$, $\alpha_\rho = \alpha_c = \alpha_\tau = 0$, $R = 55$), respectively. (c) and (d) ρ and N for space gradient driven growth ($\alpha_\rho = 1$, $\alpha_c = \alpha_n = \alpha_\tau = 0$, $R = 18$), respectively. (e) and (f) ρ and N for growth given by velocity fluctuations (pure increase of density; $\alpha_\tau = 1/9$, $\alpha_\rho = \alpha_n = \alpha_c = 0$, $R = 20$), respectively. N is given in number of tips per unit volume.

Figure 1.

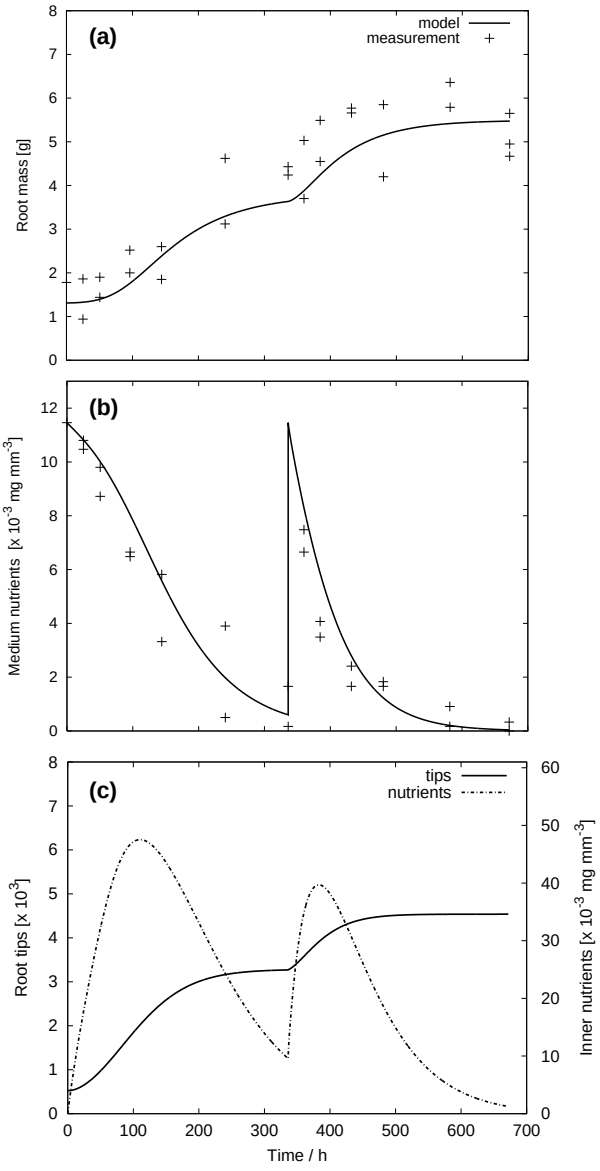
(a)
model
measurement
Root mass [g]
(b)
Medium nutrients [x 10^-3 mg mm^-3]
(c)
tips
nutrients
Root tips [x 10^3]
Inner nutrients [x 10^-3 mg mm^-3]
Time / h

Figure 2.

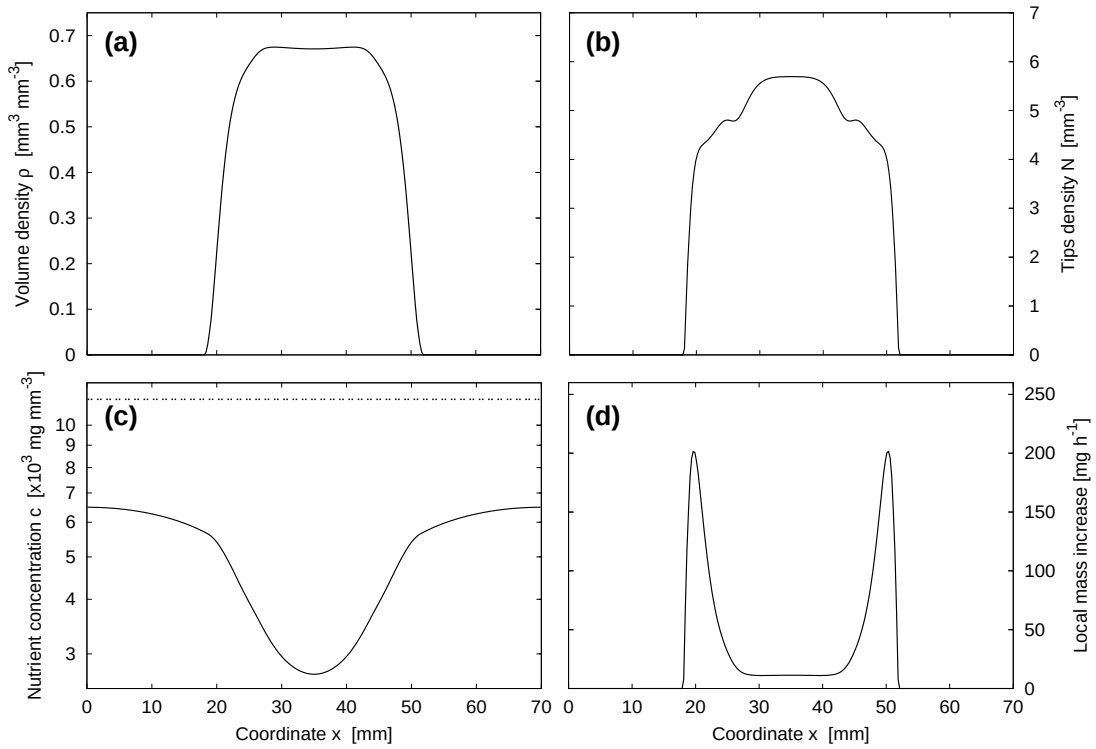
(a)
(b)
(c)
(d)
Volume density ρ [mm3 mm-3]
Tips density N [mm-3]
Nutrient concentration c [x10^3 mg mm-3]
Local mass increase [mg h-1]
Coordinate x [mm]
Coordinate x [mm]

Figure 3.

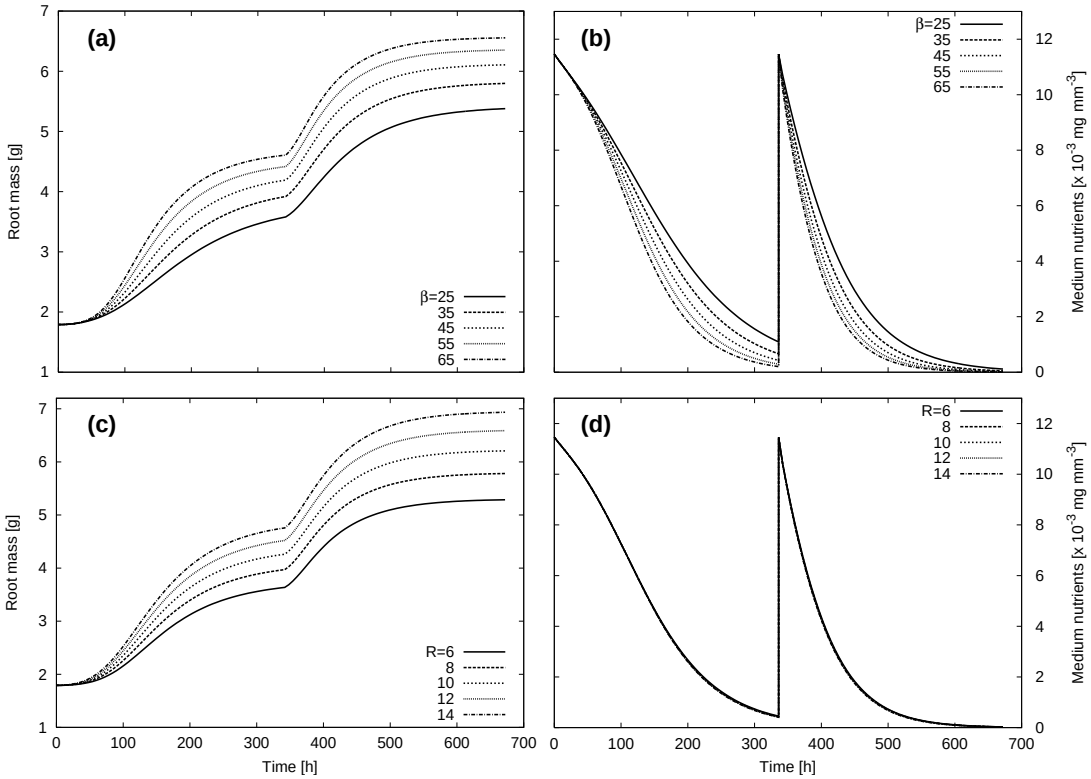
(a)
(b)
(c)
(d)
Root mass [g]
Time [h]
Medium nutrients [x 10-3 mg mm-3]
β=25
35
45
55
65
R=6
8
10
12
14

Figure 4.

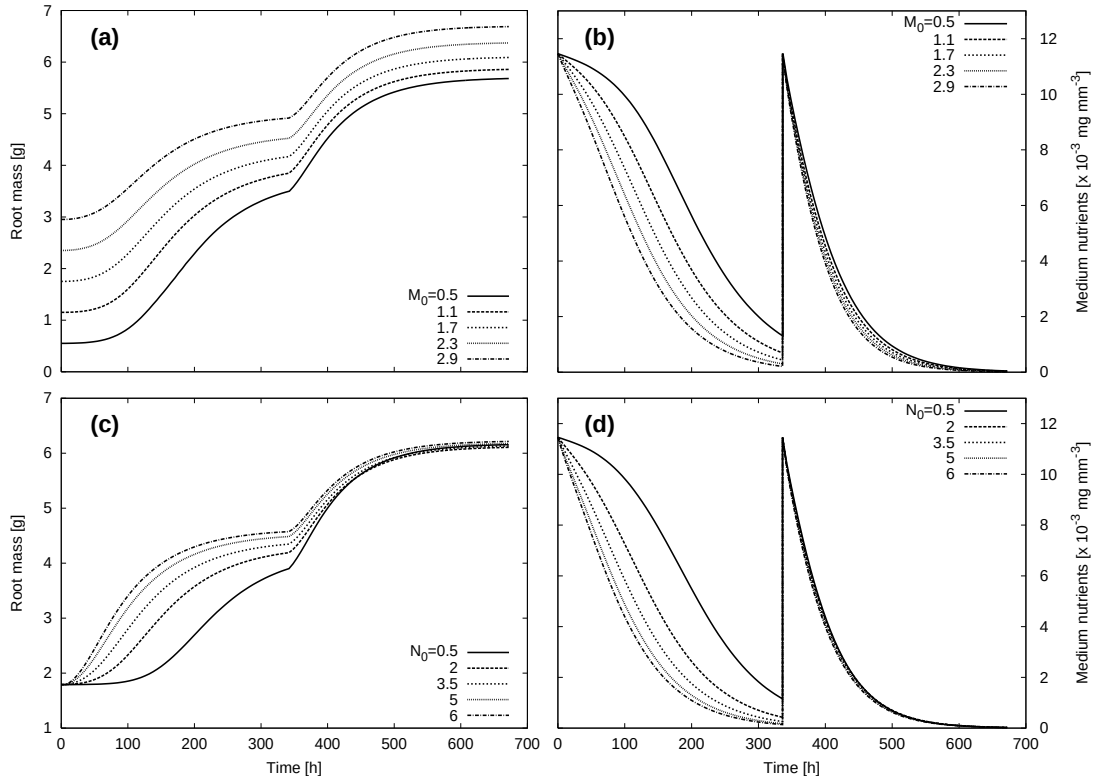
(a)
(b)
(c)
(d)
Root mass [g]
Medium nutrients [x 10-3 mg mm-3]
Time [h]
M0=0.5
1.1
1.7
2.3
2.9
N0=0.5
2
3.5
5
6

Figure 5.

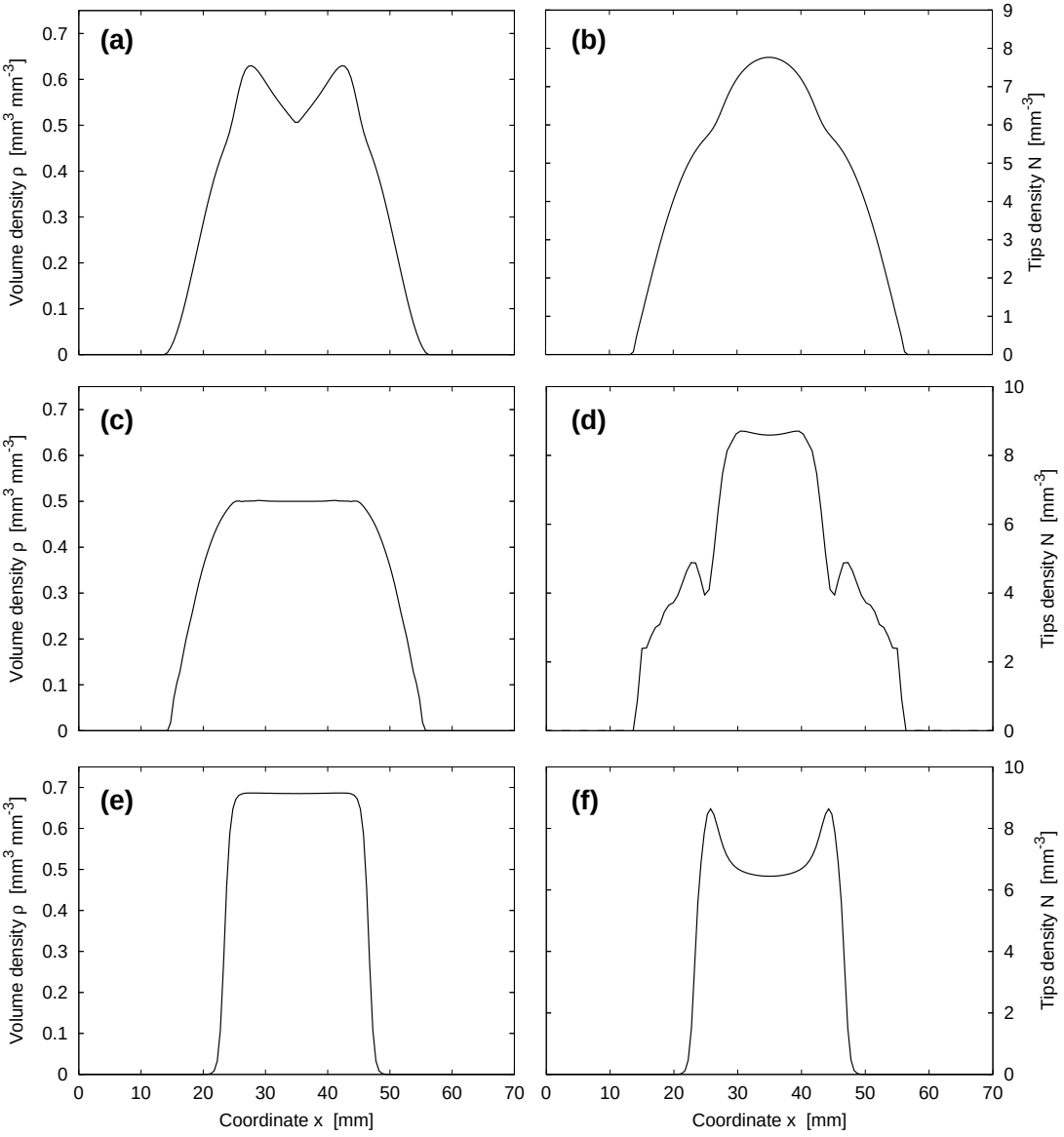
(a)
(b)
(c)
(d)
(e)
(f)
Volume density ρ [mm3 mm-3]
Tips density N [mm-3]
Coordinate x [mm]
0
0.1
0.2
0.3
0.4
0.5
0.6
0.7
1
2
3
4
5
6
7
8
9
10
20
30
40
50
60
70

Figure 6.